



Evaluation and multi-objective optimization of nose wear, surface roughness and cutting forces using grey relation analysis (GRA)

Gaurav D. Sonawane¹ · Vikas G. Sargade¹

Received: 23 February 2019 / Accepted: 28 October 2019 / Published online: 12 November 2019
© The Brazilian Society of Mechanical Sciences and Engineering 2019

Abstract

Dual-phase structure with 1:1 ratio of austenite and ferrite is termed as “Duplex”. Lower cost of duplex stainless steel (DSS) with a combination of good strength and corrosion resistance in a critical environment is captivating many applications. This research work highlights the experimental study of effect of cutting parameters such as cutting speed, feed rate, AlTiN and AlTiCrN-coated tools on response parameters, viz. tool life, surface roughness and cutting forces. Multi-objective optimization using grey relation analysis (GRA) was done to optimize quality response characteristics. High-power impulse magnetron sputtering was used to deposit AlTiN and AlTiCrN coatings on tungsten carbide substrate. Performance measures such as tool life, surface roughness and cutting forces were measured during dry turning of DSS2205 and optimized using Taguchi’s GRA technique. AlTiCrN-coated tools exhibited the best results followed by AlTiN-coated tools and uncoated tools. Tool life achieved with AlTiCrN-coated tools is 7 times more than uncoated tools, in which surface roughness was found to be reduced by 67% and cutting forces by 25%. Weighted GRG grade shows that for all the tools used, a cutting speed of 100 m/min and feed rate of 0.12 mm/rev provided optimum results for response parameters. For change in weightage to response characteristics, different optimum conditions were found for all the tools used. AlTiCrN-coated tool with 100 m/min cutting speed and 0.12 mm/rev feed rate performed better with the highest tool life, the least surface roughness and cutting forces. The results were confirmed by S/N ratio plots.

Keywords DSS2205 · HiPIMS · Characterization · Dry turning · GRA · S/N ratio

List of symbols

$X_i(k)$	Sequence after the data preprocessing
$\Delta_{0i}(k)$	Deviation sequence of the reference sequence
$\zeta_i(k)$	Grey relation coefficient
T_s	Deposition temperature of the coating
$X_i^0(k)$	Original sequence
ζ	Identification coefficient
γ_i	Grey relation grade
T_m	Melting temperature of coating

1 Introduction

The term “Duplex” is due to the dual-phase structure of austenite and ferrite in equal amount. Higher nitrogen content and fine-grained structure of duplex stainless steel (DSS) are attracting many applications. Combination of high strength and higher corrosion resistance in the critical environment is showing DSS to be a great option for austenitic stainless steel (ASS) [1]. A lower percentage of nickel due to the addition of nitrogen is responsible for the lower cost of DSS without compromising mechanical and microstructural properties. The second advantage of nitrogen addition is the reduction in the rate of secretion of intermetallic phases, which are not favourable [2]. High chromium (Cr) content, sufficient molybdenum (Mo) with nickel (Ni) content and the combination of Cr, Mo and nitrogen (N) contents provide resistance in oxidizing acids, reducing acidic environment and chloride-affected pitting and crevice corrosion, respectively. High temperature and pressure with severe chemical conditions for equipment generate high possibility of corrosion. This has created

Technical Editor: Lincoln Cardoso Brandao.

✉ Gaurav D. Sonawane
gs112@rediffmail.com

¹ Dr. Babasaheb, Ambedkar Technological University, Lonere, Maharashtra 402103, India

requirement of high mechanical strength and good corrosion resistance [3]. Pitting and crevice corrosion resistance are two important properties required for applications such as marine industry, and these properties are decided on the basis of critical pitting temperature (CPT) and critical crevice temperature (CCT). CPT and CCT of DSS 2205 are well above (40–60 °C) than that of the ASS grades (0–20 °C). Pitting resistance equivalent number (PREN) is high (36) for DSS compared to ASS grades (20). ASS grades can be used in applications where a single property is required, but in places where a combination of properties is required, DSS is the best option [4].

Earlier, SS316L was called as “Marine Steel” and was used for many under seawater applications. DSS provides better protection to stress corrosion cracking (SSC) and is now famous for marine applications. Moreover, DSS is also used for seawater process piping system, heat exchangers, subsea downhole production, evaporators in seawater at low temperature, separators, pumps and in constructions where high bearing strength is required due to the combination of saline and corrosion condition [5]. Two-phase structure and different alloying elements make DSS more suitable for different applications, but diversely due to these properties, processing of DSS is more difficult. Ferrite and austenite have different hardness, so tool experiences more force than single-phase materials while machining. Combination of low thermal conductivity, high strength and toughness makes DSS very difficult to cut. One of the biggest concerns of DSS is the formation of built-up layer (BUL) during machining. Very high heat is generated at the cutting zone while machining with DSS, which results in rapid tool wear [4].

Coating with high thermal stability, hot hardness and good oxidation resistance causes the heat generated to flow to chips instead of the tool materials [6]. Commonly, chemical vapour deposition (CVD) and physical vapour deposition techniques are used to deposit coatings on a substrate. Very high operating temperature of CVD (900 °C) causes natural brittleness of coating, partially coarse grain structure, internal tensile stresses and formation of η -phase. To overcome these disadvantages, PVD coatings are developed. PVD coatings are recommended where sharp cutting edges are used [7]. Coatings deposited by PVD have reported with a lower surface roughness of the machined surface. Nanostructured coatings provide very low coefficient of friction, called self-lubricating coatings with high hardness and strength [8]. There are two ways for improving tool life while cutting difficult to cut materials, using either the coolant or coated tools with high-performance coatings. The former is mostly used in the view of taking into account the disadvantages and cost of using lubricants. Oil-based coolants or lubricants are responsible to produce unsuitable conditions during machining [9]. Also due to health issues, the use of coolant during machining is restricted [10].

Kulkarni and Sargade [11] reported better surface properties of AlTiCrN coating deposited by high-power impulse magnetron sputtering (HiPIMS) than ternary coating deposited by cathodic arc evaporation (CAE) technique. Lukasz-kowicz and Dobrzanski [8] compared TiAlSiN, CrAlSiN and AlTiCrN nano-composite coatings for structure and mechanical properties. AlTiCrN was found to be better with respect to hardness, grain size and critical load (adhesion strength). Multilayer coatings with a middle layer of Al_2O_3 do not permit to create sufficient temperature and stresses required to activate ceramic layer [12]. Nomani and Pramanik [13] compared machinability of DSS2205 with austenite steel 316L and found DSS2205 more difficult to machine since it is more sensitive to BUL formation. Rajguru and Anrunachalam [5] reported lower cutting forces and surface roughness for tools coated with PVD coating. Oliveira and Diniz [14] reported notch wear as the most common wear mechanism while dry-turning DSS. Philip and Chandramohan [15] found the feed rate to be the most dominant parameter for surface roughness and cutting force while cutting speed for tool wear. It is recommended to use lower values of DoC but not less than tool nose radius when DSS is turned dry [3]. Gutakovskis and Bunga [16] claimed two times increase in tool life due to the use of positive chip breaker geometry. Moreover, due to the use of positive chip breaker higher cutting speeds and DoC can be used so that productivity can be improved. Lauro and Brandao [17] reported reduced machining performance using minimum quality lubrication (MQL). Dry machining exhibited better results for cutting forces, surface roughness and burr formation compared to MQL. Krolczyk et al. [18] in another research work on DSS compared dry and wet machining. Tools used for dry turning performed better with a tool life of 20.8 min as compared to 7.2 min for wet cutting, i.e. 68% higher tool life achieved using dry cutting. DSS if turned with wet conditions results in a very hard surface layer called as “white layer” followed by a soft layer beneath called as “dark layer”, resulted in temper treatment, subsequently tempered martensite is formed. Compressive residual stresses were reported after dry turning of DSS, which were tensile in nature before machining.

Researchers have used either cemented carbide tools or solid carbide tools with or without coatings. Tool geometries of DNMG150608, SNMG 120408 [19] and TNMG 160408 [20] were used for machining DSS. Very few researchers [4, 15] have optimized the DSS machining with respect to output parameters. Researchers have used grey relation analysis (GRA) and analysis of variance (ANOVA) for optimization of machining process parameters and for analysing the effect of different parameters on response characteristics, respectively [21–24].

Shanmugarajan et al. [21] have used Taguchi’s GRA with ANOVA for optimization of process parameters of welding process. Moreover, researchers have attempted to assign

weightage to response parameters so as to get different optimized conditions of input parameters. Costa et al. [25] used weighted principal component analysis (WPCA) with Taguchi's S/N ratio for optimization of dry end-milling process. Senthilkumar et al. [22] have optimized EDM process using GRA with ANOVA techniques. Similar attempt was made by Ren et al. [23] so as to optimize high-speed milling process with six different carbide grade tools to optimize tool wear and surface roughness. Two-stage optimization, viz. single objective and then multi-objective optimization, was done by Meral et al. [26] so as to optimize drilling process. High-speed turning process was optimized using GRA with ANOVA for MRR, SCE and surface roughness. Optimization results obtained confirmed the effective use of GRA [24]. Bhatt and Rawal [27] reported that many researchers have used GRA as a multi-response optimization in traditional and non-traditional machining processes. Rastee et al. [4] used response surface methodology (RSM) for optimizing DSS wet turning for responses such as tool wear, cutting forces and effective power. Krolczyk and Legutko [28] used PS/DS: λ program to optimize DSS 2205 turning process by converting a polynomial nonlinear model into a linear model.

Very few researchers [24, 29–31] have attempted to optimize traditional machining process such as turning using Taguchi's GRA technique and ANOVA to find the significant effect of input parameter. Most of the researchers have used GRA with ANOVA for non-traditional machining processes [21, 22]. It is quite important for a turning process to produce a good quality surface with minimum tool wear. Moreover, due to cost, productivity is to be considered for optimization.

Industries preferred using coated carbide tools for dry machining of DSS. Use of these tools for DSS turning needs a detailed study of tool wear and wear mechanism [12]. Use of advanced coatings for dry machining of DSS is missing. It is reported that Cr can act as a lubricious layer during machining, but the use of Cr-based coating for machining DSS has not been reported. Advanced tooling and coatings are required to enhance surface finish of machined parts. Surface roughness reported for DSS2205 is in the range of 0.64–0.89 μm , which is still higher and denotes requirement for enhancement of the performance [20]. Detailed study

related to the enhancement of cutting parameters and their optimization is still a wide area open for research [32]. Many researchers have tried working on turning DSS, but no one has detailed and optimized eco-friendly process used for DSS in terms of tool life, tool wear and surface finish [12]. This defines the need for improvement in the machining conditions and their optimization. To ensure better machining performance, it is required to pay some special attention for selecting tool material, geometry, cutting parameters, coatings and their deposition techniques.

2 Materials and methods

M grades indexable inserts with ISO specification of CNMG 120408 with MF1 chip breaker to avoid BUL formation were used for straight turning of DSS2205. Nanolayered AlTiN and AlTiCrN coatings were deposited on M35-grade tungsten carbide substrates with the help of PVD high-power impulse magnetron sputtering (HiPIMS) technique from CemeCon, Germany. Characterization of deposited coatings was done by using field emission gun scanning electron microscope (JSM-7600 FEG-SEM). Coated inserts were partially cut using wire-cut EDM and then fractured to check coating thickness. Vickers HMV-2 series microhardness tester with diamond indenter was used to check the hardness of the coatings. A load of 100 g for 15 s was used. Using critical load phenomenon, adhesion of coating was tested. Both the tests were conducted for three readings, and the average is reported in this work. Measurement of wear during the experimentation was done using Nikon microscope Eclipse 50i with Nikon's CFI60 optical system. Due to the small depth of cut, nose wear was found to be the type of wear during dry turning of DSS 2205. Tool life criterion of 0.6 mm nose wear, for uneven wear, was used according to ISO 3685 (1993). Recommendations from CemeCon, Germany, were used as the basis for the selection of coating material, type and deposition technique. X-ray spectrometry, i.e. EDS analysis technique, was used for confirming the chemical composition of materials used for workpiece and coatings. EDS analysis confirmed the alloying elements of DSS2205 as shown in Table 1.

Literature review and recommendations from the International Molybdenum Association (IMoA) were used as the basis to select cutting parameters. Moreover, data from industrial survey of current manufacturers of DSS and cutting tool (SECO) were also considered for selection of cutting parameters. Selected cutting parameters and their levels are as shown in Table 2.

A machining length of 245 mm was chosen for dry turning of a round bar of size 280 * 90 mm. Surface roughness was measured using Mitutoyo SJ301 2R-C type surface roughness tester after every pass. Kistler-make 3-component

Table 1 Chemical composition of DSS2205

Chromium	Nickel	Molybdenum
22.0–23.0%	4.50–6.5 0%	3.00–3.50%
Carbon	Nitrogen	Manganese
0.030% Max	0.14–0.20%	2.00% Max

piezo-electric force dynamometer (Model 9257) was used to measure cutting forces during machining. Field emission gun scanning electron microscope (JSM-7600 FEG-SEM) was used to capture tool wear images. Requirement of high-quality products at a lower cost is creating enough pressure on manufacturing industries. Taguchi-based GRA technique of multi-objective optimization is quite helpful to find feasible solutions to justify the need of quality products at low cost [19, 33]. The grey system is one of the effective tools for representing level between white (complete information) data and black (incomplete information) data. To express correlation between white and black information, grey relation grade (GRG) called as a quality index is used. In GRA, signal-to-noise (S/N) ratio is considered as the measure of performance [34].

First, an orthogonal array, L9 in this case, is formulated. This array is then used to examine different characteristics. After experimental results are achieved, they are transformed into weighted grey relation grades. In the present work, full factorial design was used for the design of experiment (DoE). For two parameters with three levels each, number of experiments with full factorial design is as follows:

$$\text{No of experiments} = 3^2 = 9$$

Considering this, DoE is formulated for each tool. As per DoE, experiments are conducted and results are recorded, and will be called as quality characteristics hereafter. These data are first required to convert into quantitative indices by preprocessing called as normalizing of data for another analysis. Depending on the type of measured quality characteristic, there are two approaches such as “Higher the better” and “Smaller the better”. “Higher the better” approach is processed as follows:

$$X_i^*(k) = \frac{X_i^0(k) - \min X_i^0(k)}{\max X_i^0(k) - \min X_i^0(k)} \quad (1)$$

where $X_i(k)$ is the sequence after the data preprocessing, $X_i^0(k)$ is the original sequence, $\max X_i^0(k)$ is the largest value of $X_i^0(k)$ and $\min X_i^0(k)$ denotes the smallest value of $X_i^0(k)$.

Similarly, “Smaller the better” approach is processed as follows:

$$X_i^*(k) = \frac{\max X_i^0(k) - X_i^0(k)}{\max X_i^0(k) - \min X_i^0(k)} \quad (2)$$

Table 2 Cutting parameters

Parameter	Value (s)
Cutting speed (m/min)	100, 140, and 180
Feed rate (mm/rev)	0.12, 0.15, and 0.18
Depth of cut (mm)	0.8 (constant)

After data preprocessing is done, so as to express a relation between actual and ideal normalized experimental results, grey relation coefficient (GRC) is calculated as follows:

$$\xi_i(k) = \frac{\Delta_{\min} + \zeta \cdot \Delta_{\max}}{\Delta_{0i}(k) + \zeta \cdot \Delta_{\max}} \quad (3)$$

where $\Delta_{0i}(k)$ is the deviation sequence of the reference sequence. ζ is identification coefficient: $\zeta \in [0, 1]$. After grey relation coefficient is calculated, the average of GRC is taken called as grey relation grade (GRG). It is defined as,

$$\gamma_i = \sum_{k=1}^n \xi_i(k) \quad (4)$$

Various findings related to the effect of any input parameter on the output parameter are explained in the previous section of this article. Once the experimental results are obtained, the normalized sequence is formulated. Grey relation coefficient is calculated for each of the output parameters. Normalized sequence of quality characteristics is shown in Tables 3, 4 and 5 for uncoated, AlTiN and AlTiCrN-coated tools, respectively.

3 Results and discussion

3.1 Characterization

Fractograph and microstructure of AlTiN and AlTiCrN coating are as shown in Fig. 1a, b, respectively. The SEM fractograph confirmed a thickness in the range of 3.9–4.1 μm . At 20 KX magnification, both coatings showed dense columnar structure with non-porous and defect-free grain boundaries.

Scratch test showed good adhesion strength for both coatings deposited on tungsten carbide substrates. AlTiN and AlTiCrN coating showed a critical load of 89 and 110 N, respectively. After this, coatings start delaminating from the substrate. Both the coatings showed spalling as a primary mode of failure followed by chipping along the scratch path. Good adhesion strength of coatings is due to using PVD HiPIMS technique for deposition. The T_s/T_m ratio is very low for PVD HiPIMS coatings. Here, T_s is the deposition temperature of the coating and T_m is melting temperature of coating. As this ratio increases, grain size increases. PVD coatings are deposited at a low temperature so T_s/T_m ratio is low. This results in a fine-grained structure of PVD coatings with good adhesion strength. Vickers microhardness test showed that AlTiN coating is harder than AlTiCrN coating. AlTiN and AlTiCrN coatings showed a hardness of 36 and 34 GPa, respectively. Same results were found by Kulkarni and Sargade [10]. This is due to the fact that some coatings

Table 3 Weighted grey relation grade for uncoated tool

Expt. no.	Cutting speed	Feed rate	Grey relation coefficient (GRC)			Weighted grey relation grade (GRG) (tool life = 60%, surface roughness = 30%, cutting force = 10%)	Rank
			Tool life	Surface roughness	Cutting force		
1	100	0.12	1	0.360	0.662	0.774	1
2	100	0.15	0.750	0.333	0.477	0.715	2
3	100	0.18	0.600	0.298	0.329	0.566	6
4	140	0.12	0.429	0.587	0.963	0.665	4
5	140	0.15	0.375	0.481	0.810	0.533	7
6	140	0.18	0.333	0.389	0.739	0.488	8
7	180	0.12	0.375	1	1	0.69	3
8	180	0.15	0.333	0.700	0.963	0.581	5
9	180	0.18	0.300	0.57	0.928	0.444	9

Bold values indicate the highest GRG values and optimized combination of cutting speed and feed

Table 4 Weighted grey relation grade for AlTiN tool

Expt. no.	Cutting speed	Feed rate	Grey relation coefficient (GRC)			Weighted grey relation grade (GRG) (tool life = 60%, surface roughness = 30%, cutting force = 10%)	Rank
			Tool life	Surface roughness	Cutting force		
1	100	0.12	1	0.459	0.544	0.792	1
2	100	0.15	0.5	0.426	0.531	0.481	6
3	100	0.18	0.400	0.333	0.333	0.373	8
4	140	0.12	0.667	0.604	0.661	0.648	3
5	140	0.15	0.400	0.521	0.605	0.457	7
6	140	0.18	0.333	0.375	0.559	0.368	9
7	180	0.12	0.500	1	1	0.7	2
8	180	0.15	0.333	0.829	0.877	0.536	5
9	180	0.18	0.400	0.942	0.705	0.593	4

Bold values indicate the highest GRG values and optimized combination of cutting speed and feed

Table 5 Weighted grey relation grade for AlTiCrN tool

Expt. no.	Cutting speed	Feed rate	Grey relation coefficient (GRC)			Weighted grey relation grade (GRG) (tool life = 60%, surface roughness = 30%, cutting force = 10%)	Rank
			Tool life	Surface roughness	Cutting force		
1	100	0.12	1	0.71	0.374	0.85	1
2	100	0.15	0.728	0.697	0.340	0.68	2
3	100	0.18	0.616	0.333	0.333	0.503	7
4	140	0.12	0.571	0.812	0.486	0.635	4
5	140	0.15	0.534	0.79	0.436	0.601	5
6	140	0.18	0.471	0.389	0.386	0.438	8
7	180	0.12	0.421	1	1	0.653	3
8	180	0.15	0.377	0.975	0.523	0.571	6
9	180	0.18	0.333	0.573	0.493	0.421	9

Bold values indicate the highest GRG values and optimized combination of cutting speed and feed

Fig. 1 SEM fractograph and microstructure of **a** AlTiN and **b** AlTiCrN coating

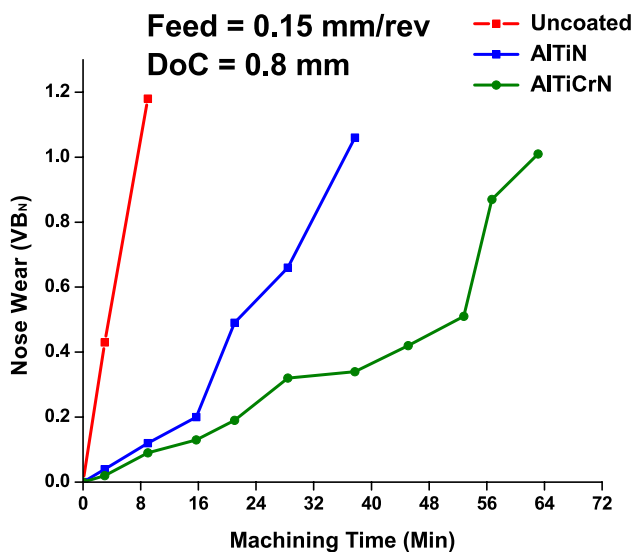
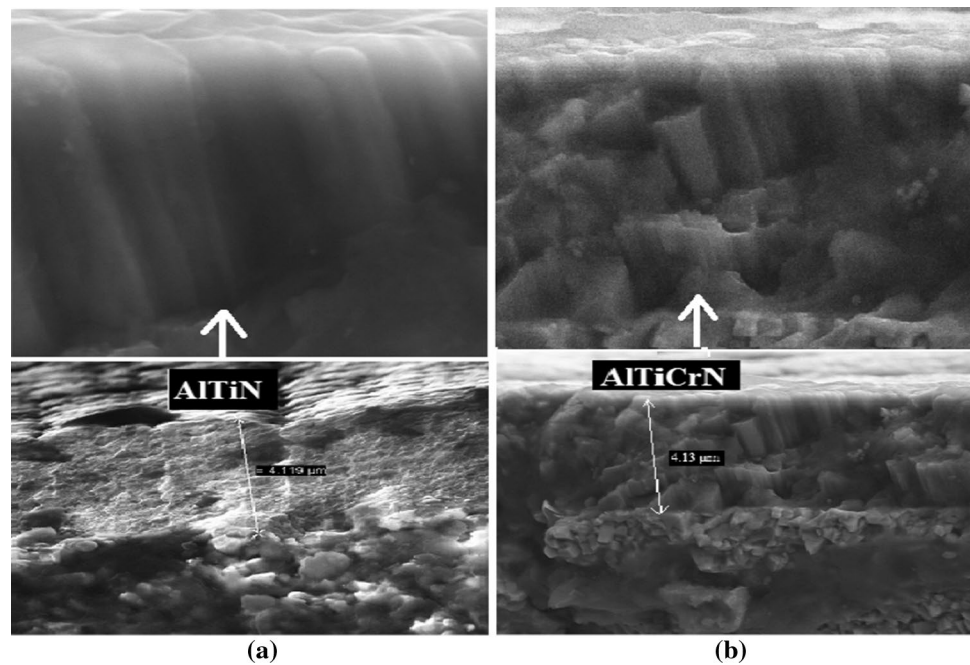


Fig. 2 Effect of machining time on nose wear

with high adhesion strength may show less hardness due to lattice orientation.

3.2 Machining performance

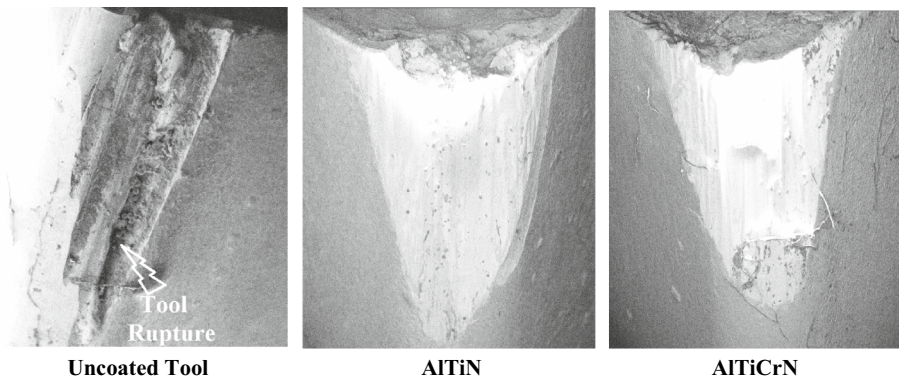
3.2.1 Effect of machining time on tool wear

Tool wear was analysed during machining of DSS2205. Nose wear was found to be the dominant wear mechanism than flank or crater wear. Effect of machining time on tool nose wear is shown in Fig. 2.

It was found that as the machining time increases, the tool wear also increases. This is due to higher temperatures produced at cutting zone [35]. This condition became more severe as more friction resulted due to increase in tool wear. Uncoated tools were unable to machine DSS2205. Uncoated cutting tools failed after a machining time of less than 9 min. Coated tools outperformed uncoated tools. At a machining time of 9 min, AlTiN and AlTiCrN-coated tools exhibited a tool wear of 0.1 and 0.08 mm, respectively. This is because of higher hardness, lower coefficient of friction, thermal stability and good adhesion of AlTiN and AlTiCrN coatings. AlTiCrN-coated tools exhibited the highest tool life of 67 min. The tool life exhibited by AlTiCrN-coated tools and AlTiN-coated tools was found to be 7 times and 4 times higher than that of the uncoated tools, respectively. Moreover, when coated tools are compared, AlTiCrN-coated tools exhibited twice the tool life of AlTiN-coated tools. This is because of the higher thermal stability of 1100 °C of AlTiCrN-coated tool as compared to 850 °C of AlTiN-coated tool [11].

Scanning electron microscopy (SEM) images of worn tools are shown in Fig. 3. Uncoated tool failed after a very short time of machining producing a notch. Rapid tool wear occurred due to the higher thermal conductivity (85–110 W/m-K) of uncoated tools than the coated tools (11–20 W/m-K). Higher thermal conductivity of uncoated tools causes most of the heat produced during machining to flow into tool material resulting in the reduction in strength of tool material, and after rapid tool wear finally chipping took place. In the case of coated tools, due to lower thermal conductivity the heat produced is carried to workpiece

Fig. 3 SEM images of worn-out tools



and chips produced [8]. AlTiN and AlTiCrN-coated tools exhibited uniform wear as shown in Fig. 3. PVD coatings are featured with retaining thermal conductivity at high temperatures due to ionic bonding. If the coating layer is chemically inert, the hardness of coating is retained even at high temperatures [5]. AlTiN coating was delaminated at 37 min of machining time, early as compared to AlTiCrN-coated tools. Cr provides more protection by forming a strong Cr₂O₃ layer. This allows AlTiCrN coating to withstand more temperatures than AlTiN coating.

3.2.2 Effect of cutting speed on surface roughness and cutting forces

Effect of cutting speed on surface roughness and cutting force is shown in Fig. 4. It was found to be significant to increase the cutting speed because as the cutting speed increases, surfaces roughness and cutting force decrease. Similar results are reported by Celik et al. [36]. This may

be due to the fact that at lower cutting speeds, the tendency of BUL formation is higher. At lower cutting speeds, friction is high and specific cutting pressure increases [37]. As a result, at lower cutting speeds higher surface roughness and cutting forces are observed.

As the cutting speed increases, BUL is reduced [38]. Due to lower BUL, friction between tool and chips produced decreases. Uncoated tools showed higher values of cutting forces and surface roughness, but the rate of reduction as the cutting speed increases is linear. Lower coefficient of friction and surface roughness of AlTiCrN coatings are the reason for less cutting forces and surface roughness of machined surface followed by AlTiN-coated and uncoated tools. Addition of Cr to coating results in the formation of a protective oxide layer which protects and helps to retain sharp edges of cutting tools even at high temperatures [11]. Also, Cr added is lubricious which reduces friction and works as a self-lubricant.

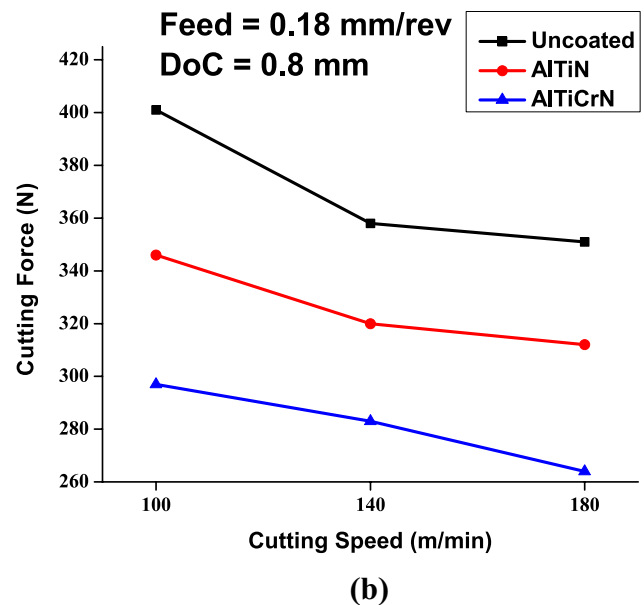
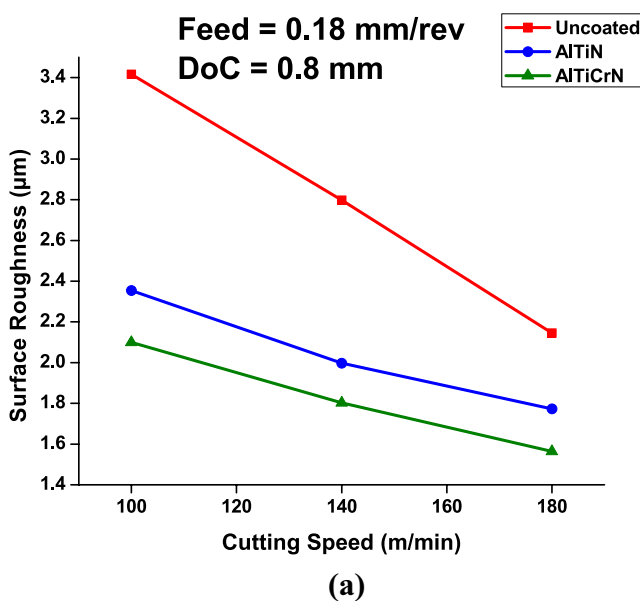


Fig. 4 Effect of cutting speed on surface roughness and cutting forces

3.2.3 Effect of feed rate on surface roughness and cutting forces

Effect of feed rate on surface roughness and cutting forces is shown in Fig. 5. At lower feed rates, less cutting forces and surface roughness were observed, and as the feed rate increases surface roughness increases. A marginal increase in cutting forces is observed with feed rate. This is due to the higher amount of materials to be removed at higher feed rates. As the feed rate increases, the friction also increases along with cutting forces and temperature in the cutting zone. Due to this, shear strength of DSS decreases and material behaves in a ductile manner. DSS itself is a sticky material and due to reduced shear strength, it becomes quite difficult to separate chips produced. Hence, at higher feed rates higher surface roughness and cutting forces are observed. Specific cutting energy tends to become constant as the cutting speed and feed rate increases. For uncoated tools, higher tool wear causes higher stresses near the cutting edges resulting in higher deformation of tool. This deformation will cause the contact between new workpiece surface and tool over very small area [39]. So, when feed rate increases, considerable amount of forces for uncoated tools is not observed to be increased at higher values of cutting speeds of 180 m/min, followed by AlTiN-coated tools.

Uncoated tools are observed with chipping failure as shown in Fig. 3 which results in more surface roughness due to high friction. AlTiN-coated tools when compared to AlTiCrN-coated tools performed poorly. This is due to lower thermal stability (850 °C) [11] and abrasion marks observed on the nose of AlTiN-coated tools.

3.2.4 Grey relation analysis (GRA)

GRA approach is applied to the normalized sequence of quality characteristics as depicted in Tables 3, 4 and 5 for uncoated, AlTiN- and AlTiCrN-coated tools, respectively.

Tool life has to be maximized, so “Higher the better” approach is used to calculate GRC for tool life. Surface roughness and cutting forces are processed for minimization. So GRC is calculated with “Smaller the better” approach for surface roughness and cutting forces. After the grey relation coefficient, grey relation grade is calculated using Eq. 4, as shown in Tables 3, 4 and 5.

It is possible to calculate grey relation grade by giving weightage to quality characteristics. Initially, GRG is calculated by giving a weightage of 60% to tool life, 30% to surface roughness and 10% to cutting forces. As productivity is a basic issue for materials such as DSS, when processed, 60% weightage is given to tool life. DSS is having many applications in the marine industry where surface roughness plays an important role just like fatigue life. So, 30% weightage is given to surface roughness. Least weightage of 10% is given to cutting force as it is having the minimum influence during the cutting process on productivity.

Grey relation coefficients of quality characteristics are summed together and are used to find weighted grey relation grade as follows:

$$\begin{aligned} \text{Weighted grey relation grade} = & (\text{Tool life GRC} * 60\%) \\ & + (\text{Surface roughness GRC} * 30\%) \\ & + (\text{Cutting force GRC} * 10\%) \end{aligned}$$

Grey relation grade for the first reading of uncoated tool is as follows:

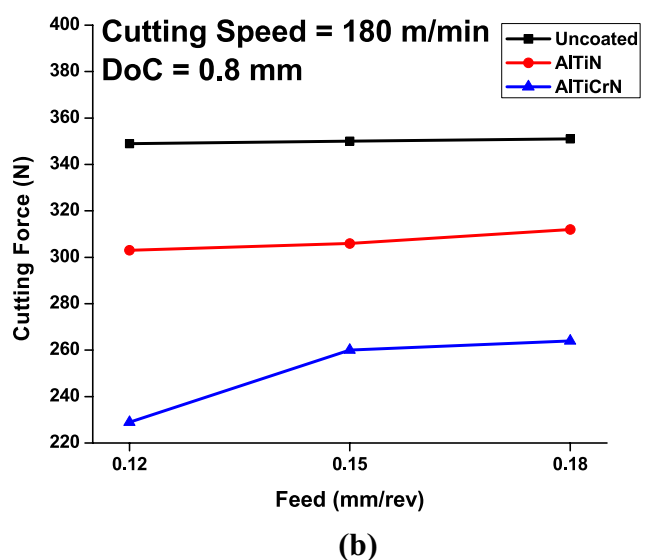
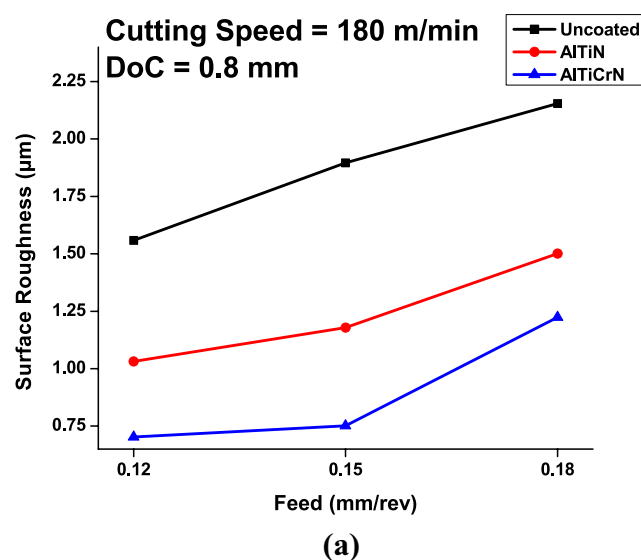


Fig. 5 Effect of feed rates on surface roughness and cutting forces

Weighted grey relation grade

$$= (1 * 0.60) + (0.360 * 0.30) + (0.662 * 0.10) = 0.774$$

Weighted grey relation grade is calculated by combining individual grey relation coefficients. Values of weighted GRG are assigned with ranks. Higher rank (1) suggests the best optimum combination of cutting parameters combined for all the quality characteristics. The lowest rank (9) shows the worst combination of cutting parameters. Scatter plot for variation of GRG for experiment number is shown in Fig. 6. The highest point shows optimum experimental parameter condition for combined results of quality characteristics. For the given weightage, all three tools used show optimum cutting speed of 100 m/min and feed rate of 0.12 mm/rev, for combined response quality characteristics such as tool life, surface roughness and cutting forces (Tables 3, 4 and 5). Weighted grey relation grade, when calculated by changing the weightage to response quality characteristics, will clearly result in different optimum input parameters. As shown in Table 6, GRG is calculated by giving a 50% weightage to both tool life and surface roughness. Optimum cutting conditions are different compared to the GRG calculations in earlier weighted GRG of 60% to tool life, 30% to surface roughness and 10% to cutting forces. Variation of assigned weightage indicated that higher cutting speeds are more suitable when uncoated and AlTiN-coated tools are used. Moreover, AlTiCrN-coated tools exhibited good machined surface quality even at low cutting speeds. This is due to lower coefficient of friction and thermal conductivity of AlTiCrN coatings used. When uncoated and AlTiN-coated tools are used at lower cutting speeds, friction between tool and the workpiece increases which causes high temperatures and

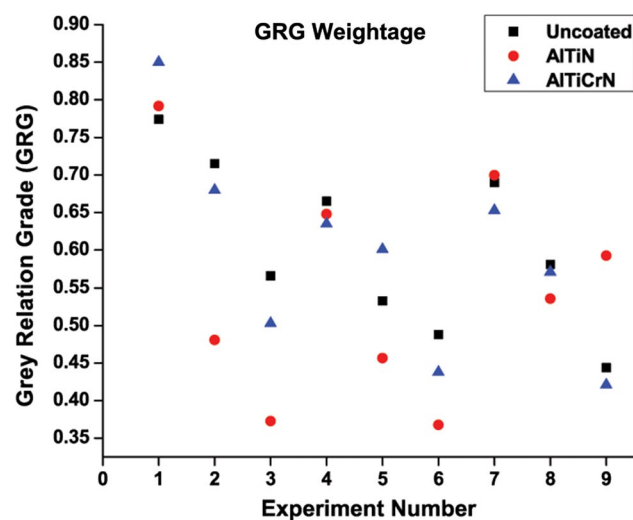


Fig. 6 Weighted GRG for 60% tool life, 30% surface roughness and 10% cutting force

Table 6 Weighted grey relation grade for 50% weightage

Expt. no.	Cutting speed	Feed rate	Weighted grey relation grade (GRG) (tool life = 50%, surface roughness = 50%, cutting force = 0%)		
			Uncoated	AlTiN	AlTiCrN
1	100	0.12	0.68	0.73	0.855
2	100	0.15	0.639	0.463	0.713
3	100	0.18	0.519	0.367	0.475
4	140	0.12	0.621	0.636	0.692
5	140	0.15	0.497	0.461	0.662
6	140	0.18	0.442	0.354	0.43
7	180	0.12	0.742	0.75	0.711
8	180	0.15	0.579	0.581	0.676
9	180	0.18	0.435	0.671	0.453

Bold values indicate the highest GRG values and optimized combination of cutting speed and feed

rapid tool wear, and as a result rough machine surface. But on the other hand, lower thermal conductivity and formation of dense Cr₂O₃ and α (Al,Cr)₂O₃ mixed oxide layer of AlTiCrN tools do not affect the surface roughness and tool wear, even when lower cutting speeds are used (Fig. 7).

Scatter plot for variation of GRG for experiment number is shown in Fig. 8. Experiment number 7 shows the highest GRG for uncoated and AlTiN-coated tools, i.e. optimized cutting conditions, whereas experiment number 1 shows the highest GRG for AlTiCrN-coated tool. For earlier model, all three tools were showing the same optimized combination of input parameters. But for 50% weightage, AlTiN-coated and uncoated tools are showing an optimized combination of cutting speed of 180 m/min with the same feed rate. This clearly suggests that one can apply different weightage to response parameters according to requirement and calculate the required optimum combination of input parameters by using grey relation analysis.

3.2.4.1 Confirmation experiment To validate the optimum input cutting conditions found using GRA analysis, a confirmation experiment was carried out for all the tools used. With the same experimental set-up and conditions, quality response characteristics were measured using a cutting speed of 100 m/min, feed rate of 0.12 mm/rev and a DoC of 0.8 mm. The results of this experiment are shown in Table 7.

It was found that values obtained with optimum cutting conditions are either closer to or better than the experimental values. These results justify the accuracy of GRA technique used for optimization of the experimental work.

3.2.4.2 Signal-to-noise (S/N) ratio Analysis of variance (ANOVA) is used to determine which input parameter is

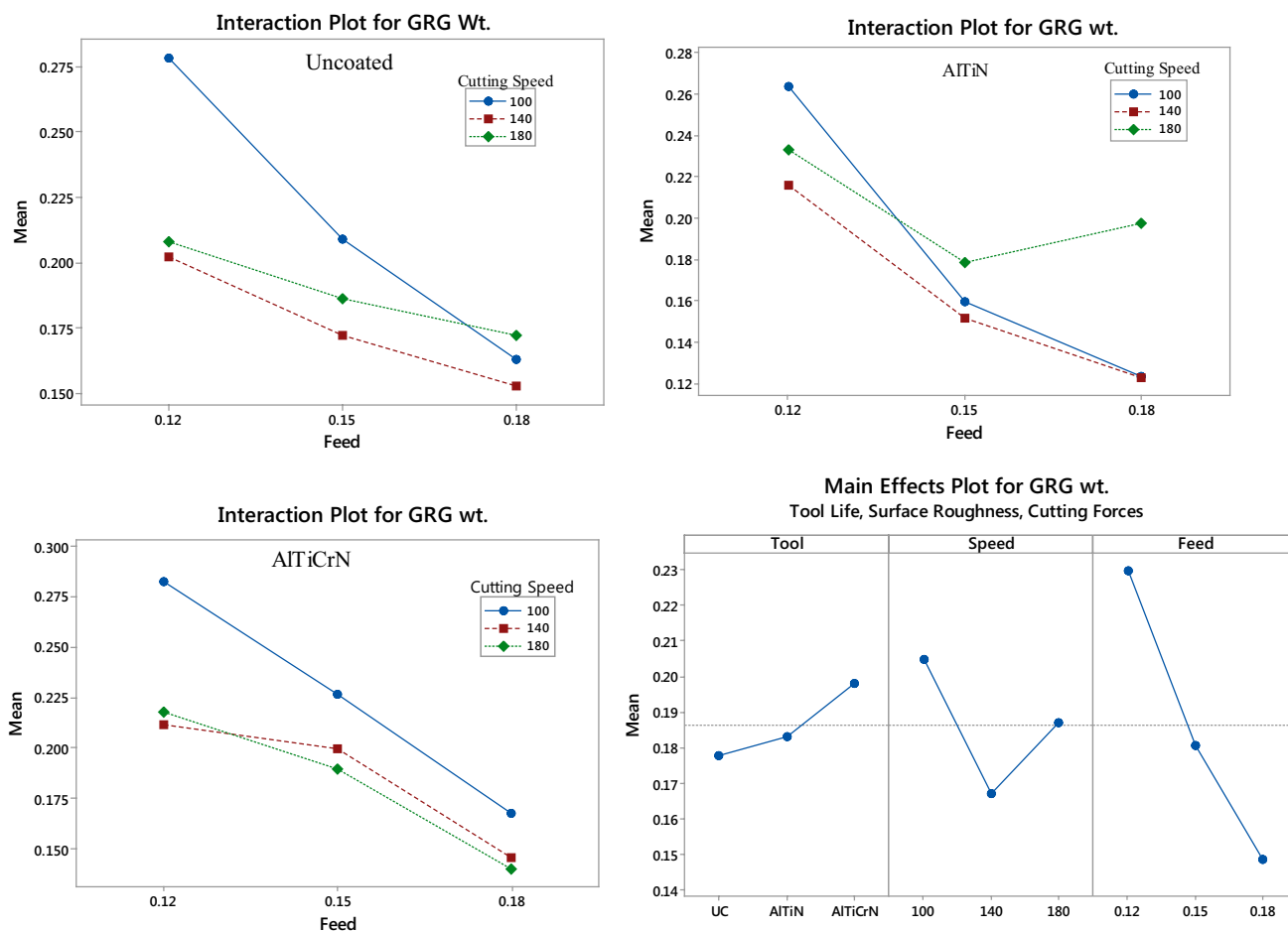


Fig. 7 Interaction and main effect plots for GRG weight

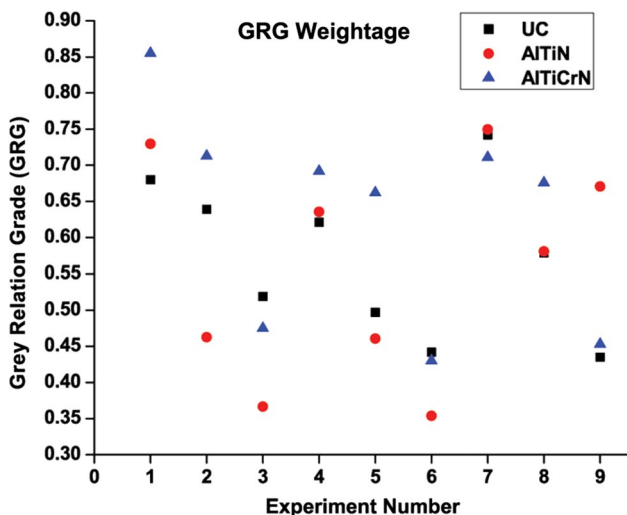


Fig. 8 Weighted GRG for 50% tool life and 50% surface roughness

Table 7 Results of confirmation experiment

	Tool life (Min)	Surface roughness (µm)	Cutting force (N)
Uncoated	40.84	2.966	358
AlTiN	87.02	1.852	322
AlTiCrN	127.60	0.962	283

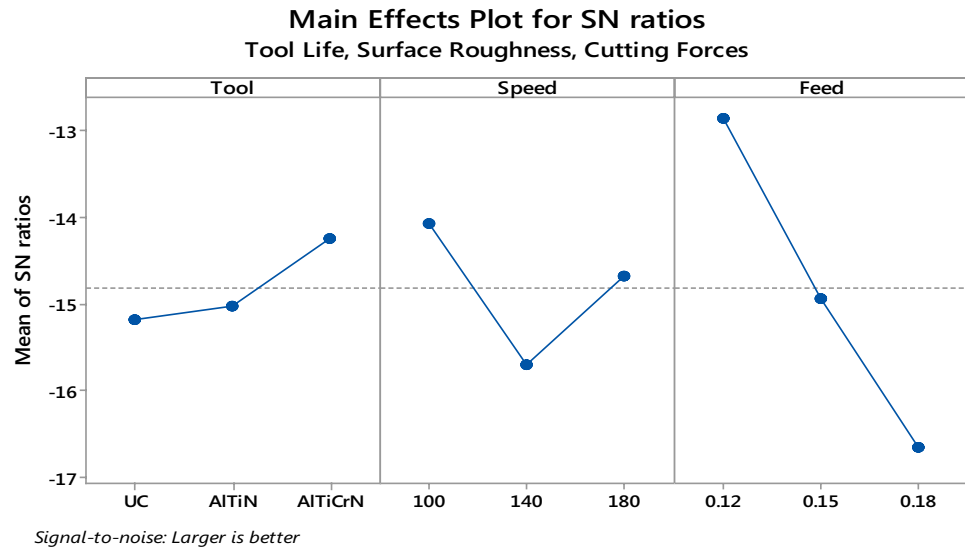
the response variable is attributed to each factor [31]. From ANOVA, it is clear that feed rate has the highest rank compared to the tool and cutting speed. So, feed rate is the most significant factor. Higher values of *F* and smaller values of *P* for feed rate than the tool and cutting speed confirm this result, as shown in Table 8. From the table, it is clear that feed rate is contributing 61.77% followed by cutting speed at 13.02% and tool with 4.14%.

ANOVA was used to confirm optimized results obtained from GRE analysis. Main effect plots for S/N ratio are as shown in Fig. 9. The results obtained by weighted GRG analysis is

having a significant effect on the response quality characteristics. Also, ANOVA suggests how much variability in

Table 8 Analysis of variance for S/N ratios

Source	DF	Seq SS	Contribution (%)	Adj. SS	Adj. MS	F value	P value
Tool	2	0.002018	4.14	0.002018	0.001009	1.96	0.166
Cutting speed	2	0.006352	13.02	0.006352	0.003176	6.18	0.008
Feed rate	2	0.030132	61.77	0.030132	0.015066	29.32	0.000
Error	20	0.010275	21.07	0.010275	0.000514		
Total	26	0.048777	100.00				

Fig. 9 Main effect plots for S/N ratios

confirmed by S/N ratio plots. S/N ratio plots are plotted with “Higher the better” criterion. Higher S/N ratio means a better condition with less vibration (noise). When higher feed rates are used due to more material to be removed, higher thermo-mechanical forces are developed [39]. This results in more vibrations, which are indicated by higher signal-to-noise ratios. Moreover, increasing cutting speed increases relative speed of sliding resulting in reduction in tool life with higher cutting speeds. Due to this, lower cutting speed and feed rates resulted as optimized cutting conditions. For results of combined quality characteristics, S/N plot also suggests the same optimized conditions, i.e. AlTiCrN-coated tool with a cutting speed of 100 m/min and feed rate of 0.12 mm/rev.

4 Conclusions

The following conclusions are drawn from the present investigation:

A. Characterization

- AlTiN and AlTiCrN deposited by HiPIMS technique showed defect-free and non-porous dense columnar structure.

- AlTiCrN exhibited higher adhesion strength than AlTiN coating. Microhardness measured for AlTiN and AlTiCrN coatings is found to be 36 GPa and 34 GPa, respectively, and thickness in the range of 3.9–4.1 μm .

B. Machining performance

- Uncoated tools showed higher tool wear for short machining time of 9 min due to increased cutting temperature, which is a result of high friction because of increased tool wear.
- Due to higher thermal stability (1100 $^{\circ}\text{C}$), AlTiCrN-coated tools exhibited the highest tool life of 63 min (7 times more than uncoated tools), followed by 38 min (4 times more than uncoated tools) by AlTiN-coated tools.
- SEM images of tool wear clearly showed tool rupture for uncoated tools and uniform wear for AlTiN- and AlTiCrN-coated tools.
- The magnitude of surface roughness and cutting forces for AlTiCrN-coated tool is found to be low followed by AlTiN-coated tools and uncoated tools due to coating properties.
- The tendency of formation of BUL at lower cutting speeds causes more surface roughness, and as the cut-

ting speed increases, lower values of surface roughness were observed due to reduced friction.

C. Grey relation analysis

- Multi-objective optimization of quality characteristics using grey relation analysis showed that a cutting speed of 100 m/min, feed rate of 0.12 mm/rev, DoC of 0.8 mm with AlTiCrN-coated tool provide optimum cutting condition during dry turning of DSS2205.
- ANOVA results indicate that feed rate is the most dominant parameter for combined quality characteristics results. Contribution of feed rate is 61.77% followed by cutting speed 13.03% and cutting tool 4.14%.
- From weighted grey relation-grade calculations, it was found that the optimum conditions vary with weightage assigned to quality characteristics.
- The substantial interaction effect is observed between feed rate and cutting speed from an interaction plot for each tool.

Acknowledgements The authors would like to express their gratitude to CemeCon, Germany, for providing timely support for coating of cutting tools.

Funding This work was supported by the NEB and Department of Science and Technology (DST), Govt. of India, under the Grant Ref: 11/10/2015-NEB (G)/03 Dated 27/09/2017.

Compliance with ethical standards

Conflict of interest The authors declare that there is no conflict of interest and authors have full control of all the data included in the manuscript, and authors agree to allow journals to review their data, if required.

Ethical standard The manuscript does not contain any clinical studies or patient data.

References

1. Asif MM, Kulkarni AS, Sathya P (2016) Optimization of process parameters of friction welding of UNS S31803 duplex stainless steels joints. *Adv Manuf* 4(1):55–65
2. Krolczyk GM, Gajek M, Legutko S (2013) Effect of the cutting parameters impact on tool life in duplex stainless steel. *Tehnicky Vjesnik (Tech News)* 20(4):587–592
3. Gamarra AR, Diniz AE (2018) Taper turning of super duplex stainless steel: tool life, tool wear and workpiece surface roughness. *J Braz Soc Mech Sci Eng* 40(39):1–13
4. Rastee DK, Heisel U, Eisseler R, Schmauder S (2014) Modeling and optimization of turning duplex stainless steel. *J Manuf Process* 16:451–467
5. Rajguru JR, Anrunachalam N (2017) Coated tool performance in dry turning of super duplex stainless steel. In: 45th SME NAMR conference, NAMRC 45, LA USA, 4–8 June
6. Stanislav V (1998) New development in super-hard coatings: the super-hard nanocrystalline-amorphous composites. *Thin Solid Films* 317:449–454
7. Bunshah RF (2002) *Handbook of hard coatings*. William Andrew Publishing, New York
8. Lukaszewicz K, Dobrzański LA (2010) Micro-structure and mechanical properties of nanocomposite coatings deposited by cathodic arc evaporation. *J Achiev Mater Manuf* 42(1–2):156–163
9. Pusavek F, Krajnik P, Kopac J (2010) Transitioning to sustainable production e-part I: application on machining technologies. *J Clean Prod* 18:174–184
10. Shashidhara YM, Jayaram SR (2010) Vegetable oils as a potential cutting fluid: an eutectic. *Tribology* 43:1073–1081
11. Kulkarni AP, Sargade VG (2015) Characterization and performance of AlTiN, AlTiCrN, TiN/TiAlN PVD coated carbide tools while turning SS304. *Mater Manuf Process* 30:748–755
12. Krolczyk G, Nieslony P, Legutko S (2015) Determination of tool life and research wear during duplex stainless steel turning. *Arch Civ Mech Eng* 15:347–354
13. Nomani J, Pramanik A, Hilditch T (2013) Machinability study of first generation duplex (2205), second generation duplex (2507) and austenite stainless steel during drilling process. *Wear* 304:20–28
14. De-Oliveira JC, Diniz AE, Bertazzoli R (2013) Correlating tool wear, surface roughness and corrosion resistance in the turning process of super duplex stainless steel. *J Braz Soc Mech Sci Eng* 36:775–785
15. Selvaraj PD, Chandramohan P, Mohanraj M (2014) Optimization of surface roughness, cutting force and tool wear of nitrogen alloyed duplex stainless steel in a dry turning process using Taguchi method. *Measurement* 49:205–215
16. Gutakovskis V, Bunga G, Torims T (2010) Stainless steel machining with nano-coated duratomic cutting tools. In: 7th international DAAAM Baltic conference “Industrial Engineering”, Tallinn, Estonia, 22–24 April
17. Lauro CH, Brandão LC, Filho SH, Davim JP (2018) Behavior of a biocompatible titanium alloy during orthogonal micro-cutting employing green machining techniques. *Int J Adv Manuf Technol* 98(5–8):1573–1579. <https://doi.org/10.1007/s00170-018-2352-8>
18. Krolczyk GM, Nieslony P, Maruda RW, Wojciechowski S (2016) Dry cutting effect in turning of a duplex stainless steel as a key factor in clean production. *J Clean Prod* 30:1–12
19. Bouchak TB, Germain G (2010) High pressure water jet assisted machining of duplex SS: machinability and tool life. *Int J Mater Form* 3(1):507–510
20. Selvaraj PD, Chandramohan P (2010) Influence of cutting speed, feed rate and bulk texture on the surface finish of nitrogen alloyed duplex stainless steels during dry turning. *Sci Res Eng* 2:453–460
21. Shanmugarajan B, Shrivastava R, Sathya P, Buvanashakaran G (2016) Optimization of laser welding parameters for welding of P92 material using Taguchi based grey relational analysis. *Def Technol* 12:343–350
22. Senthilkumar TS, Muralikannan R (2019) Enhancing the geometric tolerance of aluminum hybrid metal matrix composite using EDM process. *J Braz Soc Mech Sci Eng* 41(41):1–15. <https://doi.org/10.1007/s40430-018-1553-2>
23. Ren J, Zhai Z, Shi K, Zhou J, Yang J, Cai J (2018) Tool determination and geometry parameter optimization of carbide tool in high-speed milling of third-generation γ -TiAl alloy. *J Braz Soc Mech Sci Eng* 40(491):1–13. <https://doi.org/10.1007/s40430-018-1408-x>

24. Warsi SS, Mujtaba HA, Ahmad R, Imran SH, Khan M (2019) Sustainable turning using multi-objective optimization: a study of Al 6061 T6 at high cutting speeds. *Int J Adv Manuf Technol* 100:843–855. <https://doi.org/10.1007/s00170-018-2759-2>
25. Costa MD, Belinato G, Brito TG, Paiva AP, Ferreira JR, Balstrassi PP (2016) Weighted principal component analysis combined with Taguchi's signal-to-noise ratio to the multiobjective optimization of dry end milling process: a comparative study. *J Braz Soc Mech Sci Eng* 39(5):1663–1681. <https://doi.org/10.1007/s40430-016-0614-7>
26. Meral G, Sarıkaya M, Mia M (2019) Multi-objective optimization of surface roughness, thrust force, and torque produced by novel drill geometries using Taguchi-based GRA. *Int J Adv Manuf Technol* 101:1595–1610. <https://doi.org/10.1007/s00170-018-3061-z>
27. Bhatt RJ, Rawal HK (2018) Investigation on flow forming process using Taguchi-based grey relational analysis (GRA) through experiments and finite element analysis (FEA). *J Braz Soc Mech Sci Eng* 40(531):1–24
28. Krolczyk GM, Legotko S, Gajek M (2013) Predicting the surface roughness in dry machining of duplex stainless steel. *Metallurgia* 52(2):259–262
29. Santhanakumar M, Adalarasan R, Siddharth S (2017) An investigation on surface finish and flank wear in hard machining of solution treated and aged 18% Ni maraging steel. *J Braz Soc Mech Sci Eng* 39(6):2071–2084. <https://doi.org/10.1007/s40430-016-0572-0>
30. Eskandari B, Davoodi B, Ghorbani H (2018) Multi-objective optimization of parameters in turning of N-155 iron-nickel-base superalloy using gray relational analysis iron-nickel-base superalloy using gray relational analysis. *J Braz Soc Mech Sci Eng* 40(233):1–12
31. de Oliveira JA, Filho SH, Lauro CH, Brandão LC (2017) Analysis of the micro turning process in the Ti–6Al–4V titanium alloy. *Int J Adv Manuf Technol* 92(9–12):4009–4016. <https://doi.org/10.1007/s00170-017-0449-0>
32. Senthilkumar N, Tamizharasan T, Anandakrishnan V (2014) Experimental investigation and performance analysis of cemented carbide inserts of different geometries using Taguchi based grey relational analysis. *Measurement* 58:520–536
33. Malik A, Manna A (2018) Multi-response optimization of laser-assisted jet electrochemical machining parameters based on gray relational analysis. *J Braz Soc Mech Sci Eng* 40(148):1–21
34. Mukharjee I, Ray PK (2006) A review of optimization techniques in metal cutting processes. *Comput Ind Eng* 50:15–34
35. Rastee DK, Heisel U, Schmauder S, Eisseler R (2014) Experimental investigation and multiobjective optimization of turning duplex stainless steels. *Int J Manuf Eng* 1:1–13. <https://doi.org/10.1155/2014/921081>
36. Celik YH, Kilickap E, Guney M (2017) Investigation of cutting parameters affecting on tool wear and surface roughness in dry turning of Ti–6Al–4V using CVD and PVD coated tools. *J Braz Soc Mech Sci Eng* 39:2085–2093
37. Jebraj V, Ajaykumar L, Deepak CR, Aditya KV (2017) Weldability, machinability, and surfacing of commercial duplex stainless steel AISI 2205 for marine application. *J Adv Res* 8:183–199
38. Bordinassi EC, Frances S, Gilmar FB, Sergio D (2006) Superficial integrity analysis in a super duplex stainless steel after turning. *J Achiev Mater Manuf Eng* 18(1–2):335–338
39. Knight WA, Boothroid G (2006) Fundamentals of metal machining and machine tools. CRC Press Taylor and Francis Group, New York

Publisher's Note Springer Nature remains neutral with regard to jurisdictional claims in published maps and institutional affiliations.